

# Palladium–Allyl Complexes Based on 3,17-Dioxo-4-androstene. The Solid-State Structure of $[\text{Pd}(\eta^3\text{-C}_{19}\text{H}_{29}\text{O}_2)(\text{R-Binap})]\text{PF}_6$

Dario Drommi, Reinhard Nesper, Paul S. Pregosin,\* Gerald Trabesinger, and Fabio Zürcher

Laboratorium für Anorganische Chemie, ETH Zürich, Universitätstrasse 6, CH-8092 Zürich, Switzerland

Received April 16, 1997<sup>®</sup>

Several  $\pi$ -allyl compounds of the form  $[\text{Pd}(\eta^3\text{-C}_{19}\text{H}_{29}\text{O}_2)(\text{bidentate})](\text{anion})$ , derived from 3,17-dioxo-4-androstene, have been prepared (bidentate = *R*-Binap, **3a**; *S,S*-Chiraphos, **3b**; (6,6'-dimethoxybiphenyl-2,2'-diyl)bis(3,5-di-*tert*-butylphenylphosphine), MeO-Biphep, **3c**; the *P,S*-chelate (2,3,4,6-tetra-*O*-acetyl-1-(2-diphenylphosphino)benzylthio)- $\beta$ -D-glucopyranose, **7**, phenanthroline, **8**, and neocuproin, **9**). The solid-state structure of  $[\text{Pd}(\eta^3\text{-C}_{19}\text{H}_{29}\text{O}_2)(\text{R-Binap})]\text{PF}_6$  has been determined by X-ray diffraction methods. It is suggested that **3a** (and presumably other relatively large allyl complexes) accommodates the two large ligands by both hinging the allyl plane away from the Binap and rotating the allyl ligand. Selected aspects of the solution dynamics for **3a**, **3c**, and **9** have been followed by NOESY methods. Allyl <sup>13</sup>C NMR data are reported for the complexes.

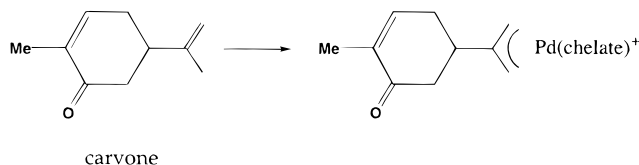
## Introduction

The chemistry of  $\pi$ -allyl–palladium complexes continues to attract interest in that these molecules provide useful preparative tools.<sup>1</sup> A variety of Pd–allyl complexes are isolable and readily accommodate both mono- and bidentate phosphine and nitrogen compounds as accompanying ligands.<sup>1–4</sup>

In the enantioselective allylic alkylation reaction, phosphine, pyrazole, and oxazoline complexes have been employed as auxiliaries, among others, with varying degrees of success in terms of enantioselectivity.<sup>5–14</sup> In this area, one finds an increasing amount of literature concerned with defining the “chiral pocket” experienced by the coordinated allyl ligand.<sup>7b,13a,14</sup> In effect, this

refers to the steric interactions between sections of the coordinated allyl and, e.g., the phosphorus substituents. These steric effects will depend on the size and bite angle of the chelate as well as its 3-D structure.

Intuitively, one would expect that the structure of the allyl must also be an important factor in determining enantioselectivity, in addition to the nature of the chelate; however, there is relatively little on the effect of allyl size in the literature. We have recently shown<sup>15</sup> that the organic allyl derived from the diterpene carvone is still quite modest in size and in terms of its solution dynamics behaves like a 2-methylallyl ligand.



We report here the synthesis and study of some chiral Pd(II)–allyl–phosphine complexes derived from 3,17-

\* Abstract published in *Advance ACS Abstracts*, August 15, 1997.

(1) Trost, B. M.; van Vranken, D. L. *Chem. Rev.* **1996**, *96*, 395. Trost, B. M. *Chemtracts: Org. Chem.* **1988**, *1*, 415. Trost, B. M.; Strege, P. E.; Weber, L.; Fullerton, T. J.; Dietsche, T. J. *J. Am. Chem. Soc.* **1978**, *100*, 3407. Trost, B. M. *Acc. Chem. Res.* **1980**, *13*, 385. Trost, B. M.; Strege, P. E. *J. Am. Chem. Soc.* **1975**, *97*, 2534.

(2) Bäckvall, J. E.; Castaño, A. M. *J. Am. Chem. Soc.* **1995**, *117*, 560. Bäckvall, J. E.; Nilsson, Y. I. M.; Andersson, P. G. *J. Am. Chem. Soc.* **1993**, *115*, 6609. Granberg, K. L.; Bäckvall, J. E. *J. Am. Chem. Soc.* **1992**, *114*, 6858. Bäckvall, J. E.; Grennberg, H.; Langer, V. *J. Chem. Soc., Chem. Commun.* **1991**, 1190. Bäckvall, J. E.; Nordberg, R. E.; Zetterberg, K.; Åkermarck, B. *Organometallics* **1983**, *2*, 1625.

(3) Norrby, P. O.; Åkermarck, B.; Haeflner, F.; Hansson, S.; Blomberg, M. *J. Am. Chem. Soc.* **1993**, *115*, 4859. Åkermarck, B.; Hansson, S. *J. Am. Chem. Soc.* **1990**, *112*, 4587. Braun, M.; Opdenbusch, K.; Unger, C. *Synlett* **1995**, 1174. Vicart, N.; Gore, J.; Cazes, B. *Synlett* **1996**, 850.

(4) Ramdehul, S.; Barloy, L.; Osborn, J.; De Cian, A.; Fischer, J. *Organometallics* **1996**, *15*, 5442.

(5) Reiser, O. *Angew. Chem.* **1993**, *105*, 576. Hayashi, T. In *Catalytic Asymmetry Synthesis*; Ojima, I., Ed.; VCH Publishers, Inc.: New York, 1993; p 325. Mackenzie, P. B.; Whelan, J.; Bosnich, B. *J. Am. Chem. Soc.* **1985**, *107*, 2046. Auburn, P. R.; Mackenzie, P. B.; Bosnich, B. *J. Am. Chem. Soc.* **1985**, *107*, 2033.

(6) Brown, J. M. *Chem. Soc. Rev.* **1993**, *25*. Brown, J. M.; Hulmes, D. I.; Guiry, P. J. *Tetrahedron* **1994**, *50*, 4493.

(7) (a) Pfaltz, A. *Acc. Chem. Res.* **1993**, *26*, 339. (b) von Matt, P.; Lloyd-Jones, G. C.; Minidis, A. B. E.; Pfaltz, A.; Macko, L.; Neuburger, M.; Zehnder, M.; Rüegger, H.; Pregosin, P. S. *Helv. Chim. Acta* **1995**, *78*, 265.

(8) Rieck, H.; Helmchen, G. *Angew. Chem.* **1995**, *107*, 2881. Knühl, G.; Sennhenn, P.; Helmchen, G. *J. Chem. Soc., Chem. Commun.* **1995**, 1845.

(9) Williams, J. M. J. *Synlett* **1996**, 705. Frost, C. G.; Williams, M. J. *Synlett* **1994**, 551.

(10) Hiraswa, K.; Kawamata, M.; Hiroi, K. *Yakugaku Zasshi* **1994**, *114* (2), 111. Yamaguchi, M.; Shima, T.; Hida, M. *Tetrahedron Lett.* **1990**, *31*, 5049. Yamaguchi, M.; Shima, T.; Yamagishi, T.; Hida, M. *Tetrahedron: Asymmetry* **1991**, *2*, 663.

(11) Tanner, D. *Angew. Chem., Int. Ed. Engl.* **1994**, *106*, 625.

(12) Togni, A.; Venanzi, L. M. *Angew. Chem.* **1994**, *33*, 497. Togni, A.; Burckhardt, U.; Gramlich, V.; Pregosin, P.; Salzmann, R. *J. Am. Chem. Soc.* **1996**, *118*, 1031. Abbenhuis, H. C. L.; Burckhardt, U.; Gramlich, V.; Koellner, C.; Pregosin, P. S.; Salzmann, R.; Togni, A. *Organometallics* **1995**, *14*, 759. Togni, A. *Tetrahedron: Asymmetry* **1991**, *2*, 683.

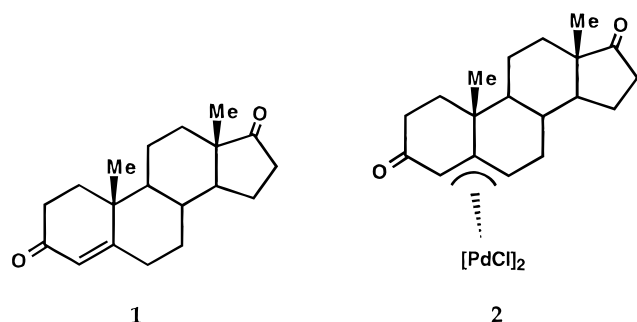
(13) (a) Pregosin, P. S.; Salzmann, R. *Coord. Chem. Rev.* **1996**, *155*, 35. (b) Albinati, A.; Pregosin, P. S.; Wick, K. *Organometallics* **1996**, *15*, 2419. (c) Barbaro, P.; Currao, A.; Herrmann, J.; Nesper, R.; Pregosin, P. S.; Salzmann, R. *Organometallics* **1996**, *15*, 1879. (d) Herrmann, J.; Pregosin, P. S.; Salzmann, R.; Albinati, A. *Organometallics* **1995**, *14*, 3311.

(14) (a) Barbaro, P.; Pregosin, P. S.; Salzmann, R.; Albinati, A.; Kunz, R. W. *Organometallics* **1995**, *14*, 5160. (b) Rüegger, H.; Pregosin, P. S. *Magn. Reson. Chem.* **1994**, *32*, 297. (c) Pregosin, P. S.; Salzmann, R. *Magn. Reson. Chem.* **1994**, *32*, 128. (d) Pregosin, P. S.; Rüegger, H.; Salzmann, R.; Albinati, A.; Lianza, F.; Kunz, R. W. *Organometallics* **1994**, *13*, 5040. (e) Rüegger, H.; Kunz, R. W.; Ammann, C. J.; Pregosin, P. S. *Magn. Reson. Chem.* **1992**, *29*, 197. (f) Ammann, C. J.; Pregosin, P. S.; Rüegger, H.; Albinati, A.; Lianza, F.; Kunz, R. W. *J. Organomet. Chem.* **1992**, *423*, 415. (g) Albinati, A.; Kunz, R. W.; Ammann, C.; Pregosin, P. S. *Organometallics* **1991**, *10*, 1800.

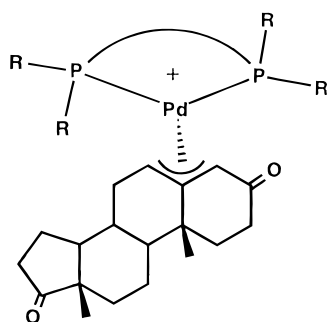
dioxo-4-androstene, **1**. This precursor was selected expecting that the allyl complexes which arise would be sufficiently large such that selective steric interactions between the allyl and various different chiral auxiliaries would be detectable. Further, these complexes might provide yet another opportunity to compare interactions from several known chiral bidentate auxiliaries, e.g., Binap and Chiraphos.

## Results and Discussion

Compound **1** is readily converted into the dinuclear chloro-bridged  $\pi$ -allyl complex **2**, which then affords cationic derivatives of the type  $[\text{Pd}(\text{allyl})(\text{bidentate})]\text{X}$  via the  $\text{TiX}_3$ - or  $\text{AgX}$ -assisted bridge-splitting in the presence of 2 equiv of the appropriate chelate. The



products **3a–c** contain the chelating phosphines, *R*-Binap, *S,S*-Chiraphos, and a methoxy-Biphep, **4** (see Chart 1), and have the general form **5**.



These complexes contain the  $\eta^3\text{-C}_{19}\text{H}_{29}\text{O}_2$  allyl ligand with the orientation of the P-substituents as shown in **5** for an *R*-Binap complex. For comparison purposes, we also prepared the thio-sugar-phosphine cation  $[\text{Pd}(\eta^3\text{-C}_{19}\text{H}_{29}\text{O}_2)(\mathbf{6})]^+$ , **7**, as well as the two cations,  $[\text{Pd}(\eta^3\text{-C}_{19}\text{H}_{29}\text{O}_2)(\text{phenanthroline})]^+$ , **8**, and  $[\text{Pd}(\eta^3\text{-C}_{19}\text{H}_{29}\text{O}_2)(\text{neocuproin})]^+$ , **9**, containing bidentate nitrogen ligands.

**X-ray Structure of 3a.** The solid-state structure of  $[\text{Pd}(\eta^3\text{-C}_{19}\text{H}_{29}\text{O}_2)(\text{R-Binap})]\text{PF}_6$ , **3a**, was determined by X-ray diffraction methods. Figure 1 shows an ORTEP view of the cation. The plot reveals that the allyl face remote from the steroid methyl groups is that which coordinates to palladium, as expected on steric grounds. The immediate coordination sphere of the metal consists of the three allyl carbons (C61–C63) and the two phosphorus donor atoms. The cation co-crystallizes with 1.5 molecules of methylene chloride.

A list of selected bond lengths and bond angles is given in Table 1, and experimental parameters for the

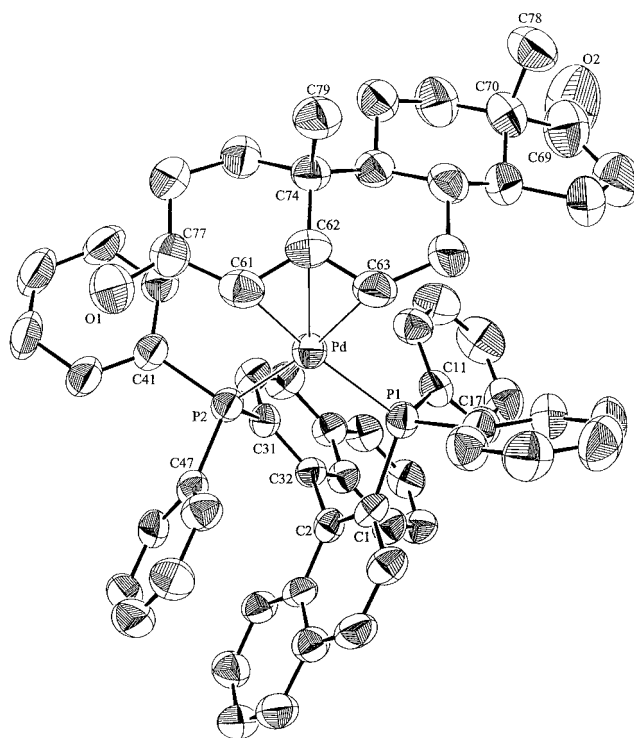
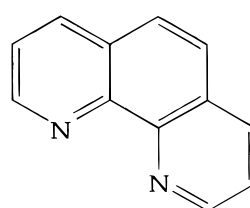
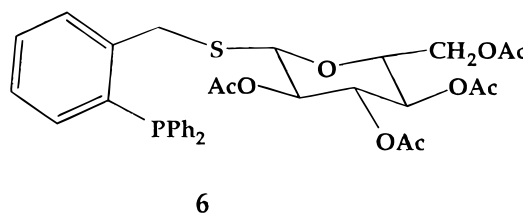
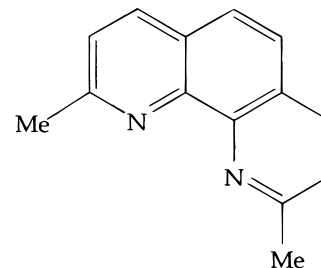


**Figure 1.** ORTEP plot for the  $[\text{Pd}(\eta^3\text{-C}_{19}\text{H}_{29}\text{O}_2)(\text{R-Binap})]^+$  cation of **3a**. Displacement ellipsoids are plotted for a 50% probability.



phenanthroline



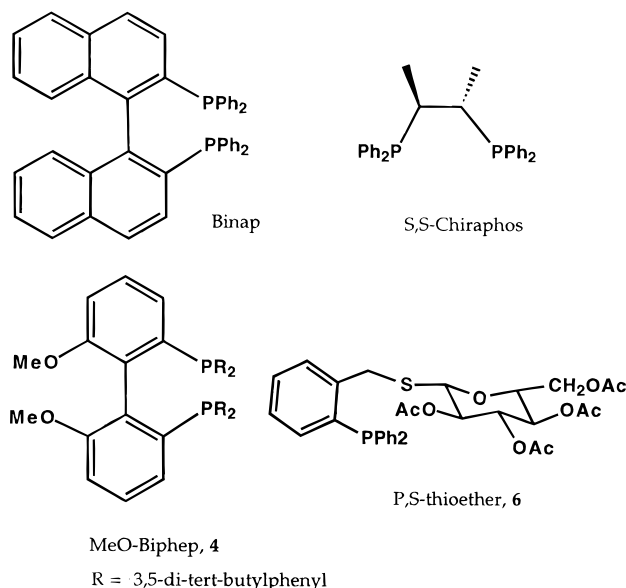
neocuproin

structure determination are given in Table 2. We have previously<sup>14d</sup> determined the structures of two allyl Pd–Binap complexes  $[\text{Pd}(\eta^3\text{-C}_{10}\text{H}_{15})(\text{S-Binap})]\text{CF}_3\text{SO}_3$ , **10**, and  $[\text{Pd}(\eta^3\text{-C}_6\text{H}_9)(\text{R-Binap})]\text{CF}_3\text{SO}_3$ , **11**, containing the  $\beta$ -pinene and *exo*-methylenecyclopentene allyl ligands. Details of these structures, together with related data from **3a**, are given in Chart 2.

For **3a**, the two Pd–P separations, 2.319(2) and 2.326(2) Å, are not significantly different and fall in the range expected for Pd–P bond lengths in allyl complexes of Pd(II).<sup>12–16</sup> The three Pd–C(allyl) distances, 2.197(6), 2.282(5), and 2.243(6) Å (C61–C63, respectively), are also consistent with the known allyl literature,<sup>12–14,16</sup> although the terminal Pd–C61 bond (proximate to the carbonyl) is significantly shorter than the terminal Pd–C63 bond. The P–Pd–P angle, 93.56(6)°, is somewhat opened but as expected for a Pd(Binap) complex.

(15) Kositzyna, N.; Antipin, M.; Lyssenko, K.; Pregosin, P. S.; Trabesinger, G. *Inorg. Chim. Acta* **1996**, 250, 365.

Chart 1. Chiral Phosphines

Table 1. Selected Bond Lengths (Å) and Bond Angles (deg) for **3a**

bond lengths		bond angles	
Pd–P1	2.319(2)	P1–Pd–P2	93.56(6)
Pd–P2	2.326(2)	C61–C62–C63	116.5(5)
Pd–C61	2.197(6)	C61–Pd–C63	65.8(2)
Pd–C62	2.282(5)	P1–Pd–C61	158.7(2)
Pd–C63	2.243(6)	P1–Pd–C63	96.9(2)
P1–C1	1.834(5)	P2–Pd–C61	103.2(2)
P1–C11	1.810(6)	P2–Pd–C63	168.9(2)
P1–C17	1.802(6)	C41–P2–C47	104.5(2)
P2–C31	1.824(5)	C31–P2–C47	106.6(2)
P2–C41	1.811(5)	C31–P2–C41	104.5(2)
P2–C47	1.793(5)	C1–P1–C17	105.1(2)
C61–C62	1.422(9)	C11–P1–C17	106.4(3)
C62–C63	1.415(9)	C1–P1–C11	107.4(3)

Interestingly, the ca. 125° angle between the allyl plane (defined by the three allyl carbons) and the P–Pd–P coordination plane is relatively large.<sup>12–16</sup> The analogous angles for the Binap complexes **10** and **11** are 121° and 122°, suggesting that **3a** avoids some steric congestion by “hinging” the allyl plane with its large organic moiety away from the P–Pd–P plane and the Binap. In more conventional allyl ligands, this interplane angle is often 110–115°.<sup>16</sup>

The relative positions of the phenyl P–C(*ipso*) Binap carbons represent one way of identifying its chiral pocket.<sup>14a</sup> These distances from the P–Pd–P plane, shown in Chart 3, help us to define the pseudoaxial and pseudoequatorial nature of the substituents. As can be seen from Chart 3 (which also gives analogous values for **10**, in which there is some asymmetry), the Binap is “normal” with all of the phenyl substituents assuming classical pseudoaxial and pseudoequatorial positions. In terms of the chiral pocket, it is worth noting that the pseudoaxial phenyl substituents are bent back away

Table 2. Crystallographic Data for **3a**

formula	C <sub>63</sub> H <sub>57</sub> O <sub>2</sub> P <sub>2</sub> PdPF <sub>6</sub> ·1.5CH <sub>2</sub> Cl <sub>2</sub>
mol wt	1286.79
cryst dims (mm)	0.70 × 0.35 × 0.35
color	yellow, transparent
data collection <i>T</i> (K)	298
cryst syst	monoclinic
space group	<i>C</i> 2 (No. 5)
<i>a</i> (Å)	19.438(14)
<i>b</i> (Å)	12.151(5)
<i>c</i> (Å)	26.392(16)
$\beta$ (deg)	106.53(5)
<i>V</i> (Å <sup>3</sup> )	5976(6)
<i>Z</i>	4
$\rho$ (calcd) (g·cm <sup>−3</sup> )	1.430
abs coeff $\mu$ (mm <sup>−1</sup> )	0.588
<i>F</i> (000)	2636
diffractometer	Scanner STOE IPDS
radiation	Mo K $\alpha$ (graphite monochromator), $\lambda$ = 0.710 73 Å
no. of measd reflns	17 524
index ranges	−22 ≤ <i>h</i> ≤ 22, −12 ≤ <i>k</i> ≤ 12, −30 ≤ <i>l</i> ≤ 30
2 $\theta$ range (deg)	7–49
no. of indep data collected	8859 ( <i>R</i> (int) = 0.04)
no. of obsd reflns ( <i>n</i> <sub>o</sub> )	8502 ( <i>F</i> > 4 $\sigma$ ( <i>F</i> ))
no. of params refined ( <i>n</i> <sub>r</sub> )	736
weighting scheme	$w^{-1} = \sigma^2(F_o^2) + (aP)^2 + bP$
<i>R</i> <sub>w</sub> <sup>a</sup>	0.122
<i>R</i> <sup>b</sup>	0.045
GooF	1.098

<sup>a</sup>  $R = (\sum w(F_o^2 - F_c^2)^2 / \sum w(F_o^2)^2)^{1/2}$ .  $P = (F_o^2 (\geq 0) + 2F_o^2)/3$ . <sup>b</sup>  $R = \sum ||F_o| - |F_c|| / \sum |F_o|$ .

Chart 2. Bond Lengths (Å) and Angles (deg) for the Allyl–Binap Complexes **3a**, **10**, and **11**<sup>a</sup>

	<b>10</b>	<b>11-CHCl<sub>3</sub></b>	<b>3a</b>
Pd–P(1)	2.328(4)	2.332(2)	2.319(2)
Pd–P(2)	2.302(4)	2.293(3)	2.326(2)
Pd–C(1)	2.15(2)	2.22(1)	2.197(6) C61
Pd–C(2)	2.22(1)	2.21(1)	2.282(5) C62
Pd–C(3)	2.25(1)	2.23(1)	2.243(6) C63
P(1)–Pd–P(2)	94.4(1)	95.12(9)	93.56(6)
Interplane Angle			
	121	122	125

<sup>a</sup> For **10** and **11**, C(1) is trans to P(2) and C(3) trans to P(1). The Pd–C data for **3a** have no relation to the Pd–C distances for C(1)–C(3), rather these are just meant as comparison values.

from the allyl ligand and have less steric significance than the pseudoequatorial Ph groups.

The relative positions of the three allyl carbons are interesting: the two terminal allyl carbons are situated above and central allyl carbon below the P–Pd–P plane; however, the distances of the the allyl termini from this plane are quite different, so that one can consider the allyl as having been rotated with respect to the coordination plane. The larger organic fragment (connected to C63) is found “down” in the somewhat empty space between the two P–phenyls (Chart 3 shows the corresponding equatorial phenyl to be ca. 0.69 Å above the plane). This distortion is very similar to what has been observed in several 1,3-diphenyl allyl complexes of bulky chiral ligands.<sup>12–14</sup>

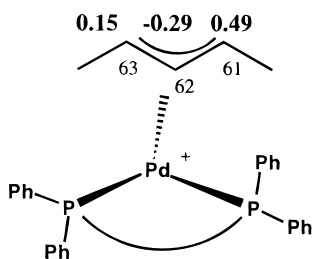
(16) Donovan, B. T.; Hughes, R. P.; Spara, P. P.; Rheingold, A. L. *Organometallics* **1995**, *14*, 489. Fernandez-Galan, R.; Manzano, B. R.; Otero, A.; Lanfranchi, M.; Pellingelli, A. *Inorg. Chem.* **1994**, *33*, 2309. Hansson, S.; Norrby, P.; Sjoegren, M. P. T.; Åkermark, B.; Cucciolito, M. E.; Giordano, F.; Vitagliano, A. *Organometallics* **1993**, *12*, 4940. Kniezinger, A.; Schöholzer, P. *Helv. Chim. Acta* **1992**, *75*, 1211. Ozawa, F.; Son, T.; Ebina, S.; Osakada, K.; Yamamoto, A. *Organometallics* **1992**, *11*, 171. Farrar, D. H.; Payne, N. C. *J. Am. Chem. Soc.* **1985**, *107*, 2054. Faller, J. W.; Blankenship, C.; Whitmore, B. *Inorg. Chem.* **1985**, *24*, 4483. Smith, A. E. *Acta Crystallogr.* **1965**, *18*, 331.

Table 3. NMR Data for **3a**, **3b**, and **3c**

	3a			3b			3c	
	<sup>1</sup> H	<sup>13</sup> C		<sup>1</sup> H	<sup>13</sup> C		<sup>1</sup> H	<sup>13</sup> C
a	4.32	78.8	a	3.88	76.5	a	4.01	80.8
b	4.43	92.4	b	4.65	92.8	b	4.04	88.4
c	1.37	26.6	c	2.27	28.2	c	1.22	27.6
c'	0.36	26.6	c'	1.20	28.2	c'	0.41	27.6
d	1.71	30.6	d	1.68	30.5	d	1.73	30.9
e	0.53	51.7	e	−0.35	50.3	e	0.65	52.1
f	1.16	21.4	f	1.32	20.6	f	1.24	21.5
f'	1.07	21.4	f'	1.42	20.6	f'	1.14	21.5
g	1.63	35.5	g	2.35	35.6	g	1.67	35.3
g'	2.22	35.5	g'	1.91	35.6	g'	2.27	35.3
h	0.72	13.6	h	0.71	13.5	h	0.74	13.7
i	1.72		i	1.67	31.0	i		
i'	1.18		i'	0.89	31.0	i'		
j	1.36		j	1.18	20.5	j		
j'	1.78		j'	1.54	20.5	j'		
k	1.10	47.9	k	0.24	46.3	k	1.10	47.2
l	1.20	20.5	l	1.19	20.6	l	1.14	20.8
m	1.93	33.3	m	1.80	33.2	m	1.64	34.9
m'	1.42	33.3	m'	1.09	33.2	m'	1.01	34.9
n	2.05	33.5	n	2.07	33.0	n	1.70	31.6
n'	1.16	33.5	n'	1.13	33.0	n'	0.17	31.6
C=O		219.0	C=O		219.2	C=O		218.5
C=O		201.0	C=O		201.2	C=O		199.9
o-α	7.14		o-α	7.61		o-α	6.52/7.71	
o-β	7.70		o-β	7.62		t-α	1.45/1.06	
o-γ	7.41		o-γ	7.76		p-α	7.65	125.9
o-δ	7.18		o-δ	7.32		o-β	7.13/7.32	127.9/129.1
						t-β	1.25/1.29	31.2/32.0
3	7.62	H <sup>a</sup>	2.99	43.4	p-β	7.60	128.6	
3'	7.84	H <sup>b</sup>	2.11	35.3	o-γ	6.79/7.39	−/132.0	
4	7.37	CH <sub>3,a</sub>	1.25	14.1	t-γ	1.19/1.31	31.4/31.6	
4'	7.74	CH <sub>3,b</sub>	1.05	14.7	p-γ	7.56	127.5	
5	7.00				o-δ	6.25/7.44		
5'	7.13				t-δ	1.40/1.14		
6					p-δ	7.54	126.1	
6'	6.71				3	6.56	115.4	
7					3'	6.54	114.3	
7'	6.92				4	7.16	129.9	
8					4'	7.01	129.1	
8'	7.12				5	7.39	123.6	
					5'	7.28	124.4	
					CH <sub>3,7</sub>	3.45	57.5	
					CH <sub>3,7'</sub>	3.30	56.8	

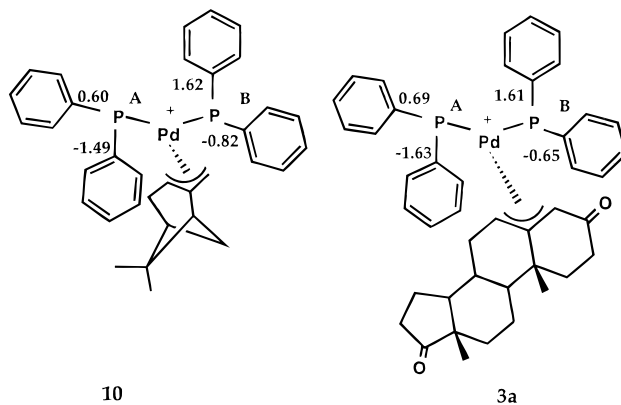
	<b>3a</b>	<b>3b</b>	<b>3c</b>
P <sup>A</sup> <sup>a</sup>	25.7	58.4	27.9
P <sup>B</sup>	22.0	50.4	23.4
<sup>2</sup> J(P <sup>A</sup> – P <sup>B</sup> )	62.7	57.8 Hz	64.4 Hz

<sup>a</sup> Chemical shifts in ppm, J-values in Hertz. P<sup>A</sup> trans to H<sup>a</sup>, P<sup>B</sup> trans to H<sup>b</sup>.



All of the bond length and bond angle data suggest that the relatively large androstene–allyl, has *no* marked effect on the Binap auxiliary. It would seem that the complex uses the hinging, together with the rotation, to comfortably accommodate the bulky chiral ligand.

**NMR Spectroscopy.** The <sup>31</sup>P NMR spectra for the bis-phosphine complexes **3a–c** reveal the expected AX or AB spin systems. Their <sup>1</sup>H NMR spectra (which are complicated, but assignable, see Tables 3–5 and Chart 4) reveal (a) that the two allyl protons are between 3.3

Chart 3. Positions of the P–C(*ipso*) Carbons Relative to the P–Pd–P Plane (Å)Table 4. NMR Data for **7** (as PF<sub>6</sub> salts)<sup>a</sup>

	<sup>1</sup> H	<sup>13</sup> C
C=O		202.2, 219.2
a	3.90	76.99
b	5.18	91.14
c	2.16	28.05
c'	0.66	28.05
d	1.78	30.70
e	-0.05	50.43
f	1.85	21.3
f'	1.33	21.3
g	2.35	35.66
g'	1.83	35.66
i	1.04	30.9
i'	1.74	30.9
k	0.67	45.70
h	0.76	13.41
l	1.39	21.45
m	2.14	33.80
m'	1.50	33.80
n	2.64	33.69
n'	2.50	33.69
o-α	7.51	135.27
m-α	7.99	130.75
p-α	7.69	133.59
o-β	7.19	134.57
m-β	7.58	130.44
p-β	7.61	133.51
9	7.59	132.80
11	7.49	133.72
12	7.03	133.82
2	5.31	67.94
3	5.43	72.98
4	4.93	68.05
5	4.04	77.83
6	4.22	62.60
6'	4.02	62.60
7	4.45	33.6
7'	4.01	33.6

<sup>a</sup> P = 22.1.

and 5.2 ppm, with H<sup>a</sup> (the proton α to the carbonyl) as a doublet, due to a <sup>31</sup>P spin, and H<sup>b</sup> as a triplet (due to one H<sup>c</sup> proton and a <sup>31</sup>P spin) and (b) that several aliphatic protons, e.g., in **3a**, **3b**, appear between ca. –0.4 and +0.6 ppm (see Figure 2) due to the anisotropy of the pseudoequatorial P–phenyl groups in these compounds.

The aromatic region of **3a** shows several broad unresolved signals which, based on 2-D exchange spectroscopy, are *not* in exchange but rather are proximate protons. We assign these two signals to the *ortho* and *meta* protons of one P–phenyl ring and conclude that the broadness results from relatively slow, but not yet restricted, rotation about one P–C bond. A similar

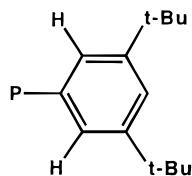
**Table 5. NMR Data for the Chelating Nitrogen Complexes (PF<sub>6</sub> salts)<sup>a</sup>**

	<b>8</b>			<b>9</b>	
	<sup>1</sup> H	<sup>13</sup> C		<sup>1</sup> H	<sup>13</sup> C
a	3.98	65.9	a	4.07	67.9
b	5.01	81.9	b	5.08	77.5
c	2.60	29.1	c	2.42	32.0
c'	1.51	29.1	c'	0.72	32.0
d	2.15	31.3	d	1.84	31.5
e	1.39	52.2	e	0.76	52.0
f	1.71	22.0	f	1.57	21.9
f'	2.27	22.0	f'	1.93	21.9
g	2.21	36.0	g	2.03	35.8
g'	2.53	36.0	g'	2.40	35.8
i	1.81	31.3	i	0.91	31.0
i'	1.20	31.3	i'	1.63	31.0
j	1.52	20.7	j	1.29	20.6
j'	1.70	20.7	j'	1.39	20.6
k	1.30	47.6	k	0.66	47.5
h	0.94	13.8	h	0.79	13.7
l	1.49	20.5	l	1.22	20.6
m	2.17	34.2	m	1.86	33.6
m'	1.91	34.2	m'	1.26	33.6
n	2.69	34.4	n	2.44	34.0
n'	2.51	34.4	n'	2.11	34.0
C=O		219.2	C=O		218.9
C=O		205.3	C=O		205.6
H21	8.56	149.81	H22	7.82	126.58
H22	8.01	126.9	H23	8.53	140.149
H23	8.73	140.7	H25	8.01	126.9
H25	8.14	128.3	H26	8.01	126.9
H26	8.14	128.3	H28	8.53	140.1
H28	8.76	140.7	H29	7.82	126.6
H29	8.17	126.9	CH3	2.98	28.7
H30	8.89	149.8			

<sup>a</sup> Nitrogen attached to C21 is trans to H<sup>b</sup>. Nitrogen attached to C30 is trans to H<sup>a</sup>.

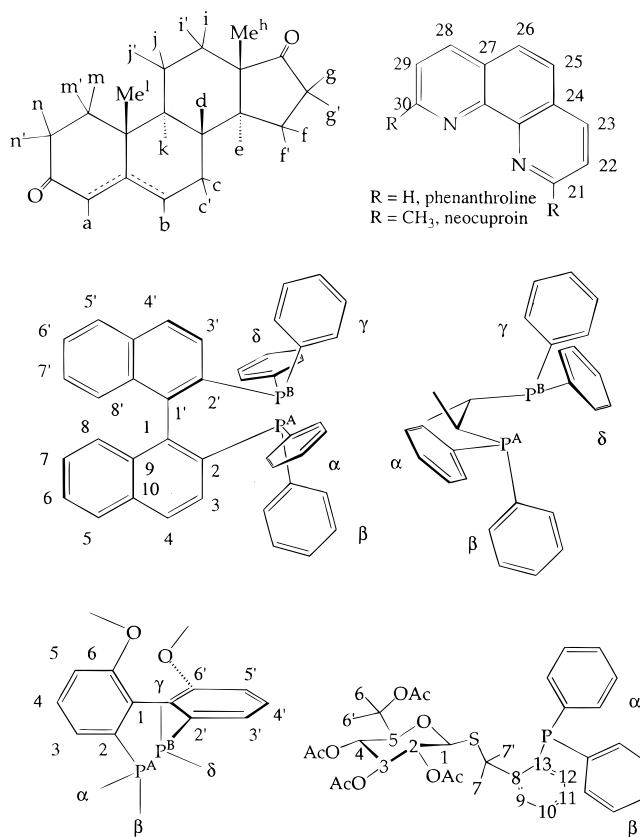
broad signal has been observed in [Pd( $\eta^3$ -C<sub>10</sub>H<sub>15</sub>)(*S*-Binap)]CF<sub>3</sub>SO<sub>3</sub>.<sup>14f</sup>

On the other hand, the NOESY spectrum in the aromatic region for the MeO-Biphep complex, **3c**, reveals two sets of *ortho* protons from the *meta*-di-*tert*-butylphenyl rings involved in a selective exchange (see Figure 3). Variable temperature measurements provide



a static spectrum at ca. 223 K, at which temperature all eight *ortho* resonances can be identified, see Figure 4. A NOESY spectrum at 213 K indicates relatively slow rotation of three of the four rings such that three pairs of selective fairly strong cross-peaks stemming from six *ortho* protons are observed. One ring is now "frozen" and its two *ortho* protons do not exchange (at least within the NMR window associated with our 0.8 s mixing time). The lack of phase distinction in this latter NOESY measurement indicates that this cation is moving relatively slowly (it is relatively large and the medium increasingly viscous). Selective NOEs from the *ortho* protons of the two pseudoequatorial aromatic rings to H<sup>c</sup> and H<sup>n</sup> suggest that the allyl in **3b** is also rotated relative to the P–Pd–P plane, as in **3a**.

The rotational barriers for the two pseudoequatorial, least hindered rings were determined via line-shape analyses using their *tert*-butyl resonances. The calcu-

**Chart 4. Numbering Schemes for the Ligands<sup>a</sup>**

$\alpha$ ,  $\beta$ ,  $\gamma$ , and  $\delta$ , in **3c** refer to the 3,5-di-*t*-butyl rings (or the Binap phenyl's).

<sup>a</sup> Primed atoms in the allyl are proximate to Pd.  $\alpha$ ,  $\beta$ ,  $\gamma$ , and  $\delta$  in **3c** refer to the 3,5-di-*tert*-butyl rings (or the Binap phenyls).

lated values of  $18.2 \pm 3$  and  $12.0 \pm 1$  kcal/mol are only estimates as these *tert*-butyl resonances are overlapped by steroid signals, thus complicating the line shapes. In any case, there are *three rings with relatively restricted rotation at ambient temperature*. In related complexes of the parent MeO-Biphep, one does not observe such restricted rotation. Warming the sample leads to coalescence of the *tert*-butyl signals, and at ca. 300 K, there are four fairly sharp singlets for the eight *tert*-butyl groups. This MeO-Biphep ligand **4** is somewhat special in that, when complexed, the *meta*-*tert*-butyl substituents make it more difficult for the phenyl rings to rotate past the biaryl moiety. Similar restricted rotation dynamics are known<sup>17,18</sup> in complexes of **4**, in particular in the allyl complex [Pd(PhCHCHCHPh)(**4**)]-PF<sub>6</sub>,<sup>19</sup> so, again, the size of the  $\eta^3$ -C<sub>19</sub>H<sub>29</sub>O<sub>2</sub> allyl is *not* primarily responsible for this behavior.

To conclude this section on the phosphine compounds: despite its relatively large size, there is no evidence, either in solution or in the solid state, for marked steric interactions between the  $\eta^3$ -C<sub>19</sub>H<sub>29</sub>O<sub>2</sub> ligand and the chiral auxiliaries. The allyl avoids this potential problem by hinging and/or rotating away from the remaining ligands.

(17) Currao, A.; Feiken, N.; Macchioni, A.; Nesper, R.; Pregosin, P. S.; Trabesinger, G. *Helv. Chim. Acta* **1996**, *79*, 1587.

(18) Feiken, N.; Pregosin, P. S.; Trabesinger, G. *Organometallics* **1997**, *16*, 537.

(19) Trabesinger, G.; Albinati, A.; Feiken, N.; Kunz, R.; Pregosin, P. S.; Tschöner, M. *J. Am. Chem. Soc.* **1997**, *119*, 6315.

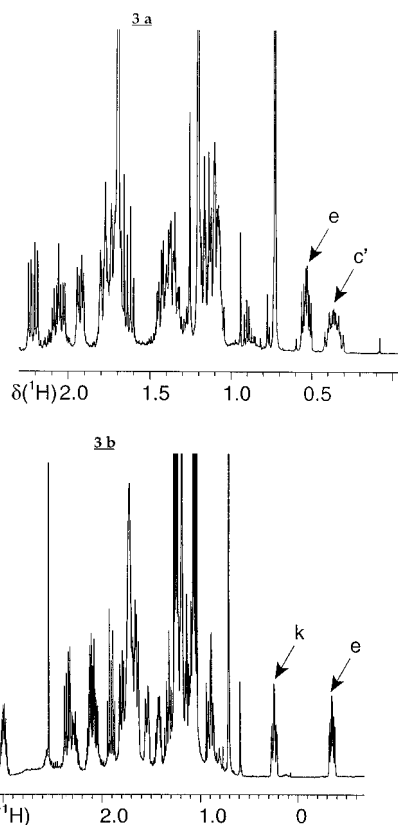


**Figure 2.** Aliphatic region of the  $^1\text{H}$  spectra of compounds **3a** and **3b**. Shielded steroid protons (indicated by arrows) are due to the proximity of one of the P–phenyl rings ( $\text{CD}_2\text{-Cl}_2$ , 500 MHz, ambient temperature).

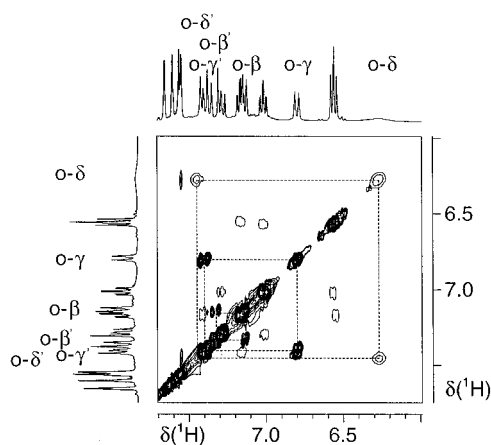


**Figure 3.** Section of the 2-D NOESY for **3c** at ambient temperature. There are four sharp *ortho* protons visible from the  $\beta$ - and  $\gamma$ -rings. The two protons from the  $\delta$ -ring are exchanging and are visible as the two very broad (not readily seen) signals. The dotted lines show exchanging pairs of protons, in one case a sharp set and in the second case a broad set ( $\text{CD}_2\text{Cl}_2$ , 500 MHz).

Room temperature NOESY spectroscopy shows that the nitrogen complexes **8** and **9** exchange the two halves of their respective  $^1\text{H}$  aromatic signals. For **8** this is a relatively slow process, with eight individual, well-resolved phenanthroline absorptions readily assigned, whereas for **9** averaging occurs relatively rapidly at ambient temperature and one observes only three aromatic signals and equivalent neocuproin methyl groups.<sup>20</sup> Line-shape analysis (between 213 and 298 K) yields an activation energy of ca.  $13.2 \pm 1$  kcal/mol for the exchange in the neocuproin derivative **9**. A very

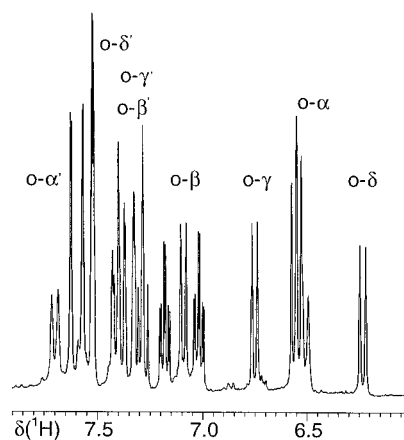
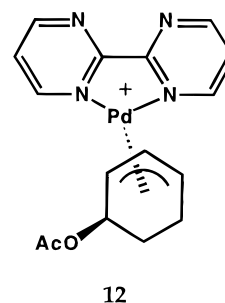


**Figure 4.** Aromatic region for **3c** at 223 K. All eight nonequivalent *ortho* protons from the four P{*m*-di-*tert*-butyl( $\text{C}_6\text{H}_3$ )} substituents are now readily observed ( $\text{CD}_2\text{-Cl}_2$ , 500 MHz).

similar value has been reported by Gogoll et al.<sup>21</sup> for the free energy of activation for the apparent ligand rotation in **12**.



In both **8** and **9** the allyl resonances are sharp. Addition of a ca. 20% excess of phenanthroline to **8** results in a marked line width increase in the aromatic region, and the 2-D exchange spectrum reveals that in addition to the intramolecular dynamics the excess and coordinated phenanthroline are also exchanging. All of the aromatic resonances now have line widths of  $\geq 30$  Hz. In the presence of excess chelate, it seems likely that this exchange is intermolecular. However, in the absence of excess ligand, an intramolecular exchange, via nitrogen dissociation in **9** to a three-coordinate complex, as suggested earlier<sup>14g</sup> and proven by Bäckvall and co-workers<sup>21</sup> for **12**, is likely given the almost identical activation energies.

To obtain some idea as to the various electronic effects exercised by the different chelates, we have recorded the  $^{13}\text{C}$  NMR spectra for our steroid complexes. Specifically, we thought it possible that the very different chiral phosphines Binap and Chiraphos might “express” themselves via their  $^{13}\text{C}$  allyl chemical shifts. For analogous  $\beta$ -pinene allyl complexes, this assumption is

(20) Although the dynamics can be complicated, allyl complexes usually rearrange via an  $\eta^3\text{-}\eta^1\text{-}\eta^3$  mechanism, see: Faller, J. W. *Determination of Organic Structures by Physical Methods*; Nachod, F. C., Zuckerman, J. J., Eds.; Academic Press: New York, 1973; Vol. 5, p 75. Vrieze, K. *Dynamic Nuclear Magnetic Resonance Spectroscopy*; Jackman, L. M., Cotton, F. A., Eds.; Academic Press: New York, 1975. Cesarotti, E.; Grassi, M.; Prati, L.; Demartin, F. *J. Organomet. Chem.* **1989**, *54*, 407. Cesarotti, E.; Grassi, M.; Prati, L.; Demartin, F. *J. Chem. Soc., Dalton Trans.* **1991**, 2073. Crociani, B.; Di Bianca, F.; Giovenco, A.; Boschi, T. *Inorg. Chim. Acta* **1987**, *127*, 169.

(21) Gogoll, A.; Oernebros, J.; Grennberg, H.; Bäckvall, J. E. *J. Am. Chem. Soc.* **1994**, *116*, 3631.

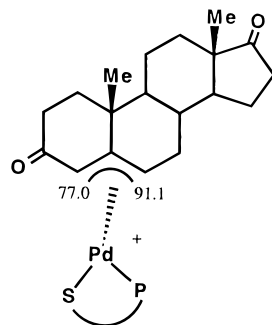
**Table 6.**  $^{13}\text{C}$  Chemical Shifts of the Terminal Allyl Carbons in the Androstene- $\eta^3\text{-C}_{19}\text{H}_{29}\text{O}_2$  Allyl Compounds

Allyl	Chelate Ligand	
$\eta^3\text{-C}_{19}\text{H}_{29}\text{O}_2$	Binap	Chiraphos
	$\delta^{13}\text{C(a)}$ 78.8 $\delta^{13}\text{C(b)}$ 92.4	$\delta^{13}\text{C(a)}$ 76.5 $\delta^{13}\text{C(b)}$ 92.8
$\eta^3\text{-C}_{19}\text{H}_{29}\text{O}_2$	MeO-Biphep, <b>4</b>	Thioether
	$\delta^{13}\text{C(a)}$ 80.8 $\delta^{13}\text{C(b)}$ 88.4	$\delta^{13}\text{C(a)}$ 77.0 $\delta^{13}\text{C(b)}$ 91.1
$\eta^3\text{-C}_{19}\text{H}_{29}\text{O}_2$	Phenanthroline	Neocuproin
	$\delta^{13}\text{C(a)}$ 65.9 $\delta^{13}\text{C(b)}$ 81.9	$\delta^{13}\text{C(a)}$ 67.9 $\delta^{13}\text{C(b)}$ 77.5
$[\text{Pd}(\mu\text{-Cl})(\eta^3\text{-C}_{19}\text{H}_{29}\text{O}_2)]_2$ , <b>2</b>		
	$\delta^{13}\text{C(a)}$ 65.8 $\delta^{13}\text{C(b)}$ 83.0	
$\eta^3\text{-C}_{10}\text{H}_{15}$ ( $\beta$ -pinene)	Binap	Chiraphos
	$\delta^{13}\text{C(1)}$ 70.3 $\delta^{13}\text{C(3)}$ 97.3	$\delta^{13}\text{C(1)}$ 62.7 $\delta^{13}\text{C(3)}$ 92.3

correct with the allyl carbons of the Binap compound at higher frequency by 5–7 ppm (see Table 6 for allyl  $^{13}\text{C}$  data).

The two resonances for the terminal allyl carbons in the  $\eta^3\text{-C}_{19}\text{H}_{29}\text{O}_2$  compounds appear between ca. 76 and 93 ppm, with the allyl carbon proximate to the carbonyl *always* at lowest frequency. If one accepts that the highest frequency is also associated with the highest relative electrophilicity, then one would predict reaction with nucleophiles only at C(b).

Strangely, for the terminal allyl carbons in **3a** ( $\delta = 78.8, 92.4$ ) and **3b** ( $\delta = 76.5, 92.8$ ), one finds <2.5 ppm separations, despite the inherent differences between these two chelates. Equally puzzling are the terminal allyl  $^{13}\text{C}$  values for the thio-sugar-phosphine complex **7**.



The structure assignment is based on selective NOEs stemming from the phosphine moiety to the steroid; however, it is not clear why this is the preferred geometric isomer. The observed terminal allyl chemical shifts, 77.0 and 91.1 ppm, are very close to those observed for the Binap and Chiraphos complexes. It seems unlikely that the thio-sugar S atom has the same donor properties as a Binap phosphorus atom,<sup>22</sup> so perhaps both *cis* and *trans* effects are operating in **7**.

When the chelate is changed to phenanthroline, i.e., complex **8**, the allyl  $\delta^{13}\text{C}$  values change by >10 ppm ( $\delta = 65.9, 81.9$ ) relative to **3a,b**. Moreover, for  $[\text{Pd}(\mu\text{-Cl})(\eta^3\text{-C}_{19}\text{H}_{29}\text{O}_2)]_2$  the chemical shifts are 65.8 and 83.0 ppm, so that the allyl carbons do show sensitivity to the remaining ligands. It is known<sup>23–25</sup> that the chemical shifts of the terminal allyl carbons depend upon the

nature of the pseudotrans donor, with tertiary phosphines resulting in higher frequency shifts relative to nitrogen donors.

**Conclusions.** The structure of **3a** has shown that allyl hinging and rotation provide two low-energy pathways via which a large allyl ligand can accommodate a sizeable chiral auxiliary, without making drastic changes in the bonding. The observed solution dynamics in **3c** and **9** suggest that the  $\eta^3\text{-C}_{19}\text{H}_{29}\text{O}_2$  allyl makes no special demands. Unexpectedly, the allyl  $^{13}\text{C}$  data for the  $\eta^3\text{-C}_{19}\text{H}_{29}\text{O}_2$  ligand are not very helpful in elucidating subtle differences, e.g., between Binap and Chiraphos (perhaps because the allyl has the degrees of freedom noted above), although these chemical shifts do show the well-known dependence on the *trans* ligand.

## Experimental Section

**General.** All reactions were performed in an atmosphere of Ar using standard Schlenk techniques. Dry and oxygen-free solvents were used. Routine  $^1\text{H}$ ,  $^{13}\text{C}$ , and  $^{31}\text{P}$  NMR spectra were recorded with Bruker 250 and 300 MHz spectrometers. Chemical shifts are given in ppm and coupling constants are given in Hertz. The two-dimensional studies ( $^1\text{H}$ , NOESY, P,H-correlation and C,H-correlation) were carried out as reported previously.<sup>13,14</sup> Elemental analyses and mass spectroscopic studies were performed at the ETHZ. We have prepared the phosphino-thioether **6** previously.<sup>13c,d</sup>

**X-ray Crystallographic Studies.** Intensity data were collected at room temperature on a STOE IPDS (image plate detector system). The program EXPOSE<sup>26</sup> was used for the data collection. The unit cell dimensions were obtained by applying the program CELL.<sup>26</sup> Finally, the data reduction was performed using CONVERT.<sup>26</sup> An internal correction of the absorption was performed with DECAY.<sup>26</sup> The structure was solved with the program SHELXS-86<sup>27</sup> using the Patterson method. Finally, the structure was refined with SHELXL-93.<sup>28</sup> Least-squares methods with anisotropic thermal parameters were used for all non-hydrogen atoms in the refinement of the compound. All hydrogen atom positions were placed in calculated positions (riding model) with fixed isotropic parameters ( $U_{\text{iso}} = 0.080 \text{ \AA}^2$ ). The positions of the solvent molecules were disordered and not completely occupied, so that there were six molecules of methylene chloride in the unit cell. The distances between the chlorine atoms and the carbon atom in the methylene chloride was held constant. Molecular graphics were performed by ORTEP II<sup>29</sup> with 50% ellipsoids.

**Synthesis of  $[\text{Pd}(\mu\text{-Cl})(\eta^3\text{-C}_{19}\text{H}_{29}\text{O}_2)]_2$ , **2**.** Commercially available 4-androstene-3,17-dione (2.54 mmol, 727 mg) was dissolved in 44 mL of dried THF.  $\text{PdCl}_2$  (1.69 mmol, 300 mg) and NaCl (6.77 mmol, 396 mg) were added, and the yellow-brown solution stirred for 7 days under reflux. The solution was filtered through Celite and transferred into 300 mL of water. The mixture was then extracted with  $5 \times 100 \text{ mL}$  of ethyl acetate. The water fraction was removed, and the ethyl acetate fraction was dried over  $\text{MgSO}_4$ . After evaporation to dryness, the orange oily residue was recrystallized at  $-20^\circ\text{C}$  from a minimum amount of  $\text{CH}_2\text{Cl}_2$  and 30 mL of hexane, followed by a second recrystallization from a minimum amount

(24) Boag, N. M.; Green, M.; Spencer, J. L.; Stone, F. G. A. *J. Chem. Soc., Dalton Trans.* **1980**, 1208.

(25) Kurosawa, H.; Asada, N. *Organometallics* **1983**, 2, 251.

(26) Scanner Stoe IPDS diffractometer software, version 1.08; Stoe & Cie: Darmstadt, Germany, 1993.

(27) Sheldrick, G. M. *SHELXS-86. Program for the Solution of Crystal Structures*; University of Göttingen: Göttingen, Germany, 1985.

(28) Sheldrick, G. M. *SHELXL-93. Program for the Refinement of Crystal Structures*; University of Göttingen, Göttingen, Germany, 1993.

(29) Larson, A. C.; Lee, F. L.; Le Page, Y.; Webster, M.; Charland, J. P.; Gabe, E. J. *NRCVAX Crystal Structure System with interactive version of ORTEP II*; NRC: Ottawa, Canada, 1986.

(22) Appleton, T.; Clark, H. C.; Manzer, L. *Coord. Chem. Rev.* **1973**, 10, 335.

(23) Åkermark, B.; Krakenberger, B.; Hansson, S.; Vitagliano, A. *Organometallics* **1987**, 6, 620.

of hot ethylester. After removing the solvent, a light-yellow-colored powder was obtained, which was dried in vacuo. Yield: 432.3 mg (60%). Anal. Calcd for  $C_{38}H_{50}Cl_2O_4Pd_2$  (854.56): C, 53.41; H, 5.90. Found: C, 52.94; H, 6.06. FAB-MS: 854.3 ( $M^{+}$ ), 819.2 ( $M^{+} - Cl$ , 100), 784.1. IR ( $cm^{-1}$ , CsI): 2939 s, 1678 s, 1637 s, 1261 m, 1222 m, 809.  $^1H$  NMR: 4.36 ( $H^b$ ), 3.34 ( $H^a$ ), 2.02 ( $H^c$ ), 1.28 ( $H^c$ ), 1.81 ( $H^d$ ), 1.27 ( $H^e$ ), 1.52 ( $H^f$ ), 1.94 ( $H^f$ ), 2.42 ( $H^g$ ), 2.06 ( $H^g$ ), 0.86 ( $H^h$ ), 1.60 ( $H^k$ ), 1.28 ( $H^i$ ), 2.40 ( $H^n$ ), 2.18 ( $H^n$ ).  $^{13}C$  NMR: 219.8, 203.4 ( $C=O$ ), 83.0 ( $C^b$ ), 65.8 ( $C^a$ ), 51.9 ( $C^e$ ), 47.7 ( $C^k$ ), 34.8 ( $H^c$  and  $C^n$ ), 31.0 ( $C^d$ ), 29.6 ( $C^g$ ), 19.8 ( $C^i$ ), 13.7 ( $C^h$ ).

#### Selected Preparative Details for the Derivatives of 2.

**Synthesis of  $[Pd(\eta^3-C_{19}H_{25}O_2)(Chiraphos)]PF_6$ , 3b.** The Cl-bridged **2** (22 mg, 0.024 mmol) was dissolved in a minimum amount of oxygen-free MeOH in an argon atmosphere. *S,S*-Chiraphos (21 mg, 0.049 mmol) was added, and within 1 min, the suspension clarified to a homogeneous yellow solution. After 10 minutes of stirring, slightly less than 1 equiv (95%) of TlPF<sub>6</sub> (16 mg, 0.046 mmol) was added, and the solution stirred for another 10 min under exclusion of light. The suspension was then filtered through Celite and evaporated to dryness. Recrystallization of the residue was achieved by first dissolving in a minimum amount of  $CH_2Cl_2$  and then slowly adding ether so that the two phases do not mix. This is followed by slow addition of an equal volume of pentane to the ether layer. The three phases mix very slowly and induce precipitation of 42 mg (90%) of the product as a yellow solid. Anal. Calcd for  $C_{47}H_{53}O_2F_6P_3Pd$  (963.27): C, 58.60; H, 5.55. Found: C, 58.61; H, 5.56. FAB-MS: 817.1 ( $M^{+} - PF_6$ , 100), 748.1, 748.9, 680.9, 590.9, 531.9, 475.8. IR ( $cm^{-1}$ , CsI): 2943 m, 1728 s, 1656 s, 1433 w, 1261 s, 1029 s, 695 m, 637. An identical procedure was employed for the Binap complex, **3a**, and this was also obtained in ca. 90% yield. Anal. Calcd for  $C_{63}H_{57}O_2F_6P_3Pd \cdot 1.5CH_2Cl_2$  (1159.47): C, 60.20; H, 4.70. Found: C, 61.48; H, 4.75. (A referee has noted that the calculated values for only one  $CH_2Cl_2$ , C, 61.77; H, 4.78, are in better agreement with the observed results).  $^{31}P$  NMR: 24.9 (d), 20.6 (d). FAB-MS: 1013.1 ( $M^{+} - PF_6$ ), 876.8, 759.2, 727.9, 655.0, 437.0. IR ( $cm^{-1}$ , CsI): 3049 m, 2944 m, 1731 s, 1672 s, 1478 w, 1435 s, 1285 s, 913 s, 696 s, 637 s.

**Preparation of  $[Pd(\eta^3-C_{19}H_{25}O_2)(R-MeO-Biphep)]PF_6$ , 3c.** The chloro-bridged dimer  $[Pd(\eta^3-C_{19}H_{25}O_2)Cl]_2$  (21.5 mg, 0.025 mmol) and the chiral phosphine *R*-MeO-Biphep (51.9 mg, 0.050 mmol) were added to 15 mL of  $CH_2Cl_2$ , and the resulting

solution was stirred for 1 h. TlPF<sub>6</sub> (17.6 mg, 0.050 mmol) in 2 mL of  $CH_2Cl_2$  was then added to the yellow solution with immediate precipitation of a white solid. The resulting suspension was stirred in the dark for a further 20 min and then filtered through Celite to remove TlCl. The filtrate which results was concentrated by distilling the solvent, and the crude product recrystallized from  $CH_2Cl_2$ /pentane. The yellow solid was washed with cold ether and dried in vacuo to afford 75.2 mg (96%) of **3c**. Anal. Calcd for  $C_{89}H_{120}O_4F_6P_3Pd$  (1567.26): C, 67.77; H, 7.55. FAB-MS: 1422 ( $M^{+} - PF_6$ , 74.6).

**Preparation of  $[Pd(\eta^3-C_{19}H_{25}O_2)(P,S\text{-ligand})]PF_6$ .** This compound was prepared by a procedure similar to that for making  $[Pd(\eta^3-C_{19}H_{25}O_2)(R-MeO-Biphep)]PF_6$  using 22.1 mg of  $[Pd(\eta^3-C_{19}H_{25}O_2)Cl]_2$  (0.026 mmol), 33.0 mg of the *P,S*-ligand (0.052 mmol), and 18.1 mg of TlPF<sub>6</sub> (0.052 mmol). Yield: 59.9 mg (98%) of a yellow powder. Anal. Calcd for  $C_{52}H_{60}O_{11}F_6P_2-SPd$  (1175.50): C, 53.13; H, 5.15. Found: C, 52.94; H, 5.07.

**Preparation of  $[Pd(\eta^3-C_{19}H_{25}O_2)(phenanthroline)]CF_3SO_3$ , 8.** The chloro-bridged dimer  $[Pd(\eta^3-C_{19}H_{25}O_2)Cl]_2$  (23.1 mg, 0.027 mmol) was added to a solution of the nitrogen chelate phenanthroline (10.7 mg, 0.054 mmol) in ca. 20 mL of  $CH_2Cl_2$ , and this was stirred for 1 h. AgCF<sub>3</sub>SO<sub>3</sub> (13.9 mg, 0.054 mmol) in 2 mL of  $CH_2Cl_2$  was then added, and the mixture was stirred for 1 h in the dark. The finely divided precipitate of AgCl was filtered through a Celite plug, and the solvent was distilled. The crude solid was recrystallized from  $CH_2Cl_2$ /ether–pentane, collected by filtration, washed with ether–pentane, and dried in vacuo. Yield: 83% (32.3 mg).

**Acknowledgment.** P.S.P. thanks the Swiss National Science Foundation and the ETH Zurich for financial support. We also thank F. Hoffmann-La Roche AG for a gift of the MeO-BIPHEP ligand as well as Johnson Matthey for the loan of the precious metals.

**Supporting Information Available:** Tables of bond lengths, bond angles, torsion angles, anisotropic displacement parameters, atomic coordinates, and hydrogen coordinates and isotropic displacement parameters (10 pages). Ordering information is given on any current masthead page.

OM9703245